15TH IEA HEAT PUMP CONFERENCE
MAY 26–29, 2026 | HOFBURG
VIENNA 2026
DECARBONISATION THROUGH INNOVATION

Performance evaluation of a novel transcritical CO_2 dual-mode ejector-enhanced cycle

Aihua Wu [a], Zian Hao [a], Jialiang Hua [a], Xingmin Wang[a], Guogeng He [a,*]

[a]School of Energy and Power Engineering, Huazhong University of Science and Technology, Wuhan 430074, China

Abstract

The development of sustainable energy technologies is crucial for mitigating climate change. Currently, the widely used hydrofluorocarbons (HFCs) pose a significant climate threat due to their high global warming potential (GWP), making their substitution particularly urgent. CO_2, as a natural, environmentally friendly, and safe working fluid, is considered one of the promising alternative refrigerants. To improve the performance of CO_2 cooling and heating, this study proposes a novel CO_2 dual-mode ejector-enhanced heat pump cycle (DEEC). This cycle operates as a dual-temperature ejector expansion refrigeration cycle in cooling mode and as an ejector-boosted heat pump in heating mode. Compared with the conventional vapor compression cycle (CVCC), the DEEC features two dedicated ejectors for the cooling and heating modes, respectively, which effectively reduces throttling losses and lowers the compressor pressure ratio, resulting in a significant improvement in cycle efficiency. Moreover, the optimized cycle configuration achieves effective thermal matching between the air and refrigerant, reducing irreversible losses during heat exchange. The performance of the DEEC was evaluated against the CVCC through energy and exergy analysis. The results demonstrate that across the studied parameter range, the DEEC shows an improvement in the coefficient of performance for cooling (COP_c) and heating (COP_h) of 22.9%-32.4% and 8.8%-13.9%, respectively, compared with CVCC. Furthermore, the exergy efficiency of the DEEC is 16.2%-20.7% higher under cooling mode and 10.6%-11.2% higher under heating mode. The proposed CO_2 ejector-enhanced cycle demonstrates promising application potential in fields requiring efficient cooling and heating, such as building spaces and vehicles.

Selection and/or peer-review under the responsibility of the organizers of the 15th IEA Heat Pump Conference 2026.

Keywords: Transcritical CO_2 cycle; Combined heating and cooling; Ejector; Performance assessment; Exergy analysis

1. Introduction

As global industrialization advances, the climate crisis driven by greenhouse gas accumulation is becoming increasingly severe. Global warming is leading to more frequent extreme weather events, whose extensive impacts threaten global ecological security and sustainable development. In response, the Kigali Amendment to the Montreal Protocol mandates a phasedown of hydrofluorocarbons (HFCs). Consequently, identifying environmentally friendly alternative refrigerants has become an urgent and critical mission for the refrigeration and heat pump industry. Currently, hydrofluoroolefins (HFOs) and hydrocarbons (HCs) have received attention due to their low global warming potential (GWP) and favorable thermophysical properties. However, a study on HFO-1234yf emissions in Europe indicated that about 30–40% of HFO-1234yf emissions are deposited as trifluoroacetic acid (TFA) within Europe, with the remainder being transported to the Atlantic Ocean, Central Asia, the North and tropical Africa [1]. Meanwhile, HCs (such as R290) exhibit high flammability, presenting substantial safety challenges for widespread application in large-scale systems [2]. In contrast, the natural refrigerant CO_2 (R744), which has a GWP of 1, an ODP of 0, and is non-toxic and non-flammable, is regarded as one of the most promising alternative refrigerants.

The substantial pressure differential across the expansion device in the transcritical CO_2 cycle results in significant throttling losses, constraining system efficiency. While both expanders and ejectors can be

* Corresponding author. *E-mail address:* gghe@mail.hust.edu.cn

employed to recover the expansion work, expanders suffer from issues such as high cost and cavitation erosion, whereas ejectors offer simplicity, low cost, and high reliability, and thus have garnered broad interest from researchers. In the CO_2 refrigeration cycle, the experimental results of Denso in 2004 showed a 25% improvement in performance of a CO_2 transcritical refrigeration system using an ejector compared to the basic system [3]. Manjili et al. [4] designed a novel two-stage transcritical CO_2 refrigeration system with dual-ejector, which showed a 20% to 80% increase in coefficient of performance (COP). Wen et al. [5] presented an improved CO_2 refrigeration cycle introducing an ejector that recovers expansion work and entrains vapor from the flash tank. Under the optimal discharge pressure, both the exergy efficiency and COP increased by 24.76%, the exergy destruction in the expansion device was 37.38% lower than that in the basic cycle. Cen et al. [6] proposed a CO_2 refrigeration cycle incorporating a dual-ejector configuration and demonstrated its advantages over single-ejector cycle through theoretical analysis. While their work provides important insights into performance improvement under cooling operation, the proposed cycle is limited to refrigeration mode and its feasibility for reversible heating operation has not been explored. Regarding heating performance, Wang et al. [7] found that the incorporation of an ejector could reduce the compressor pressure ratio significantly compared to a conventional cycle. The exergy destruction in the throttling process decreased by 95.38%–98.76%, and the COP improved by 7.38%. Xing et al. [8] proposed a novel two-stage compression CO_2 heat pump in which two ejectors were deployed in the high-pressure and low-pressure stages, respectively, to reduce the throttling losses at each stage. Under specified operating conditions, the heating capacity was enhanced by 10.5% to 30.6% compared to the basic cycle. Zou et al. [9] proposed a dual-evaporator CO_2 heat pump integrated with an ejector and an internal heat exchanger (IHX), and analyzed cycle performance under different IHX effectiveness and ejector nozzle throat areas. The results indicated that although increasing the ejector throat area would reduce the optimal COP, it amplified the positive effect of IHX on COP improvement. These studies indicate that ejectors play an important role in improving cooling or heating performance in various applications of CO_2 system.

Notably, due to the inherent unidirectional operation of ejectors, systems incorporating them generally cannot operate in reverse. Most existing research on ejector-integrated systems is confined to single-mode operation. However, in certain application scenarios such as building spaces and mobile transportation vehicles, systems often require dual-mode operation to provide efficient cooling in high-temperature conditions and heating in low-temperature conditions. Although some researchers have investigated dual-mode CO_2 systems with integrated ejectors, such as the study by Wang et al. [10] where an ejector was incorporated in cooling mode to enhance refrigeration performance, the cycle became a basic transcritical cycle without ejector in the heating mode, thereby forfeiting the performance benefits provided by this component. Simultaneous performance enhancement for both cooling and heating in direct-expansion, air-cooled CO_2 air-conditioning systems has rarely been addressed.

Based on this, this study proposes a novel transcritical CO_2 dual-mode ejector-enhanced cycle (DEEC). This cycle operates as an ejector-enhanced dual-temperature evaporation refrigeration cycle in cooling mode and as an ejector-boosted heat pump in heating mode. The introduction of the ejectors, combined with optimized cycle configuration, significantly reduces irreversibilities in both the throttling and heat exchange processes. To evaluate the application potential of the novel cycle, this study compares its performance in both cooling and heating modes with conventional single stage vapor compression cycles (CVCC) through energy and exergy analysis. It should be noted that the present study evaluates DEEC based on a small-capacity system, while the DEEC is also suitable for application in higher-capacity systems. The research findings are expected to provide valuable references for the design and performance enhancement of CO_2 cycles.

2. Cycle description

The schematic diagram of the DEEC is shown in Fig. 1. The cycle incorporates two dedicated ejectors for the cooling and heating modes, respectively, with a four-way valve enabling the switching between the operating modes. Furthermore, the dual-evaporator/gas cooler (indoor unit) is designed to reduce the heat exchange temperature difference for both the air and refrigerant in both operating modes.

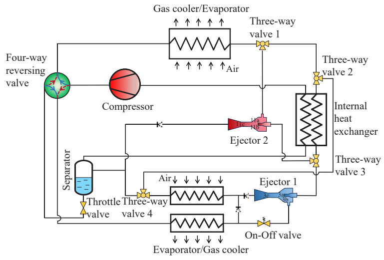

Figure 1. Schematic diagram of DEEC.

The schematic diagrams of the CVCC for cooling and heating are shown in Fig. 2. In cooling mode, the outdoor unit operates as the gas cooler while the indoor unit functions as the evaporator, these roles are reversed in heating mode. During operation, CO_2 discharged from the compressor passes through the gas cooler for cooling, the internal heat exchanger (IHX) for subcooling, and a throttling device before evaporating in the evaporator and returning to the compressor.

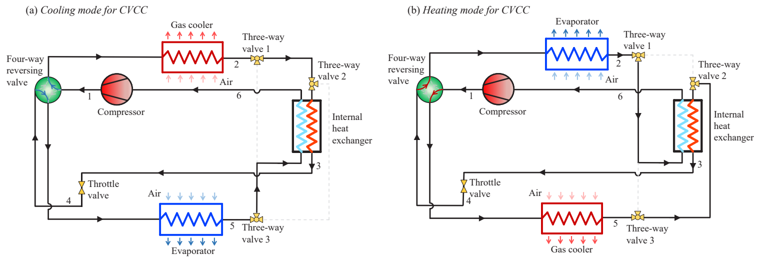

Figure 2. Schematic diagrams of CVCC for (a) cooling mode and (b) heating mode.

Fig. 3 presents the operational schematics and *T-s* diagrams of the DEEC for both cooling and heating modes. In the cooling mode, CO_2 discharged from the compressor is first cooled in the gas cooler (outdoor unit) and the internal heat exchanger (IHX). It then serves as the primary flow for ejector 1. The fluid exiting the ejector flows into the high-temperature evaporator (indoor unit) for evaporation (state points 4-5). The resulting two-phase mixture is separated in the separator. The vapor phase is routed back to the compressor, while the liquid phase is throttled and fed into the low-temperature evaporator (states 8-9) for evaporation, after which it is entrained as the secondary flow into ejector 1. In the heating mode, the high-temperature CO_2 from the compressor first releases heat in the gas cooler (indoor unit, states 1-9/4-5). After being subcooled in the IHX, it flows to ejector 2 as the primary flow. Following phase separation, the vapor returns to the compressor, and the liquid is throttled and enters the evaporator (outdoor unit). The fluid exiting evaporator is then entrained by ejector 2 as the secondary flow.

The incorporation of ejectors reduces throttling losses and increases compressor suction pressure in both operating modes. Furthermore, the pressure-boosting effect of the ejector enables dual-temperature evaporation at the indoor unit during cooling. This configuration achieves counter-flow heat exchange between the refrigerant and air in both modes, thereby reducing heat transfer irreversibility.

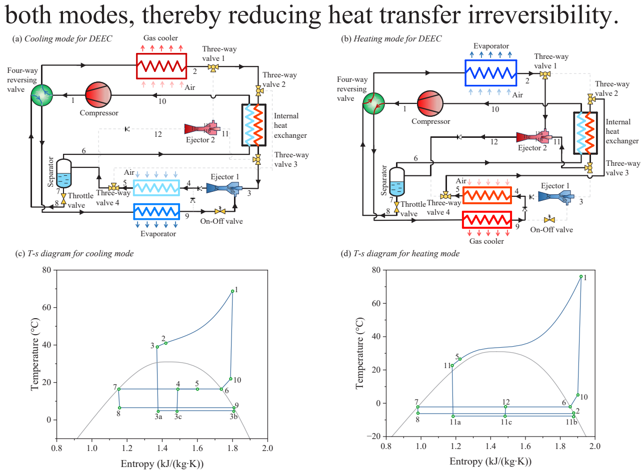

Figure 3. Operating mode schematics and *T-s* diagrams of DEEC: (a) Cooling mode schematic, (b) Heating mode schematic, (c) Cooling mode *T-s* diagram, (d) Heating mode *T-s* diagram.

3. Mathematical modeling

3.1. Energy performance model

The theoretical model is based on the following assumptions [11, 12]:
(1) The throttling process is isenthalpic;
(2) Pressure drops and heat losses in pipelines and heat exchangers are neglected;
(3) The evaporator outlet is saturated vapor;
(4) The temperature difference between the gas cooler outlet and the ambient temperature is set to 6 °C;
(5) The flow within the ejector is steady-state;
(6) Mixing of the primary and secondary flows in the ejector occurs at constant pressure.

3.1.1. Ejector model

The parameters of the fluid flowing through the various sections of the ejector are calculated as shown in Table 1.

Table 1. Calculation equations for fluid parameters at different ejector sections.

	Calculation equations
Motive nozzle	$h_{mn,out} = h_{mn,in} - \eta_{mn}(h_{mn,in} - h_{mn,out,is})$
	$c_{mn,out} = \sqrt{2(h_{\mathrm{mn,in}} - h_{mn,out})}$
Suction nozzle	$h_{sn,out} = h_{sn,in} - \eta_{sn}(h_{sn,in} - h_{sn,out,is})$
	$c_{sn,out} = \sqrt{2(h_{sn,in} - h_{sn,out})}$
Mixing chamber	$\Delta P = P_{\mathrm{sn,in}} - P_{\mathrm{m}}$
	$c_{m,out}(\dot{m}_{mn} + \dot{m}_{sn}) = \sqrt{\eta_m}(\dot{m}_{mn}c_{mn,out} + \dot{m}_{sn}c_{sn,out})$
Diffuser	$h_{d,out}(\dot{m}_{mn} + \dot{m}_{sn}) = \dot{m}_{mn}h_{mn,in} + \dot{m}_{sn}h_{sn,in}$
	$h_{d,out} = h_{m,out} + \frac{c_{m,out}^2}{2}$
	$h_{d,out,is} = \eta_d(h_{d,out} - h_{m,out}) + h_{m,out}$

The entrainment ratio μ is expressed as:

$$\mu = \frac{\dot{m}_{sn}}{\dot{m}_{mn}} \tag{1}$$

3.1.2. Thermodynamic performance model

The compressor isentropic efficiency and the IHX effectiveness are denoted by η_{com} and η_{IHX} [10]:

$$\eta_{\mathrm{com}} = 0.815 + 0.022CR - 0.0041CR^2 + 0.0001CR^3 \tag{2}$$

$$\eta_{\mathrm{IHX}} = \frac{h_6 - h_5}{h_{6t} - h_5} \tag{3}$$

where *CR* represents the compression ratio. As shown in Fig. 2(a), h_5 and h_6 are the specific enthalpies at the heated fluid inlet and outlet, respectively, while h_{6t} denotes the specific enthalpy at pressure P_6 and the cooled fluid inlet temperature.

In the calculation, the evaporator heat transfer rate is expressed as:

$$\dot{Q}_e = UA\Delta T_e \tag{4}$$

where *A* is the heat transfer area, and *U* is the heat transfer coefficient. The *UA* value remains consistent between the CVCC and DEEC. For the dual-temperature evaporation cycle, the *UA* is set to 312.5 W/K for each evaporator, at half of the total value [12]. Besides, ΔT_e represents the logarithmic mean temperature difference (LMTD) between the refrigerant and air in the evaporator, expressed as:

$$\Delta T_e = \frac{(T_{air,in}-T_e)-(T_{air,out}-T_e)}{ln\frac{(T_{air,in}-T_e)}{(T_{air,out}-T_e)}} \tag{5}$$

The heat transfer rate of air side and refrigerant side are expressed as:

$$\dot{Q} = \dot{V}_{air}\rho_{air}C_{p,air}\Delta T_{air} \tag{6}$$

$$\dot{Q} = \dot{m}(h_{out} - h_{in}) \tag{7}$$

In DEEC, the cooling capacity ratio between the medium-temperature and low-temperature evaporators is defined as CCR:

$$CCR = \frac{\dot{Q}_{e,MT}}{\dot{Q}_{e,LT}} \tag{8}$$

The COP of CVCC and DEEC is expressed as:

$$COP = \frac{\dot{Q}_{IE}}{\dot{W}_{com}} \tag{9}$$

In order to prove the advantages of DEEC over CVCC, the COP improvement ratio of DEEC over CVCC is expressed as:

$$\Delta COP = \frac{COP_{DEEC}-COP_{CVCC}}{COP_{CVCC}} \times 100\% \tag{10}$$

3.2. Exergy performance model

The exergy at a certain state point is:

$$ex = (h - h_0) - T_0(s - s_0) \tag{11}$$

where s_0 and h_0 are the specific entropy and enthalpy at the reference state (T_0 = T_{amb}, P_0 = 101 kPa), respectively.

The exergy destruction $\dot{I}$ is expressed as:

$$\dot{I} = \sum Ex_{in} - \sum Ex_{out} \tag{12}$$

The cycle total exergy destruction $\dot{I}_{tot}$ is expressed as:

$$\dot{I}_{tot} = \sum \dot{I}_i \tag{13}$$

The exergy efficiency η_{ex} is expressed as:

$$\eta_{ex} = 1 - \frac{\dot{I}_{tot}}{\dot{W}_{com}} \tag{14}$$

3.3. Model validation

The thermodynamic model of the proposed cycle is implemented and solved in Matlab. The thermophysical properties of fluid are obtained from the REFPROP 10.0. For validating the ejector model, experimental data from Zhu et al. [13] are used to compare with the simulation results. The entrainment ratio is computed under the operating conditions reported by Zhu et al., Table 2 presents a comparison of calculated versus experimental entrainment ratios. The results demonstrate that the computed entrainment ratios agree closely with the experimental values, with deviations within an acceptable range.

Table 2. CO_2 two-phase ejector model validation [13].

P_P (MPa)	T_P (°C)	P_S (MPa)	T_S(°C)	P_B (MPa)	μ_{exp}	μ_{cal}	Error (%)
8.1	35.0	3.62	22.4	4.20	0.6860	0.6758	-1.49%
8.44	35.0	3.62	22.0	4.19	0.6394	0.6327	-1.04%
8.72	35.6	3.61	20.5	4.19	0.6232	0.6377	2.32%
9.05	35.7	3.62	22.4	4.22	0.5869	0.6168	5.10%
9.19	35.2	3.60	22.8	4.27	0.5013	0.5344	6.60%
9.26	35.5	3.60	22.8	4.27	0.5112	0.5425	6.13%
8.67	35.2	3.62	22.4	4.10	0.7224	0.7721	6.88%
8.63	35.1	3.63	22.5	4.22	0.5935	0.6065	2.18%

4. Results and discussion

The rated operating conditions for CVCC and DEEC are summarized in Table 3, with the corresponding calculated results provided in Table 4. It can be observed that the DEEC achieves an increase in COP of 28.9% and in exergy efficiency of 19.5% under cooling mode, and 11.6% and 10.6%, respectively, under heating mode, compared to the CVCC. These results confirm a significant performance enhancement from the optimized cycle configuration. In the section 4.1-4.2, a detailed comparative performance analysis between the CVCC and DEEC in both cooling and heating modes will be presented based on energy and exergy analyses, aiming to further explore the potential of the DEEC.

Table 3. Operation parameters of CVCC and DEEC.

Parameters	Value
Cooling capacity $\dot{Q}_c$ (kW)	5
Heating capacity $\dot{Q}_h$ (kW)	7
Compressor discharge pressure P_{dis} (MPa)	9.5 MPa (cooling) and 7.8 MPa (heating)
Outdoor ambient temperature $T_{o,amb}$ (°C)	35 °C (cooling) and 7 °C (heating)
Indoor ambient temperature $T_{i,amb}$ (°C)	27 °C (cooling) and 20 °C (heating)
Outdoor air volume flow $\dot{V}_{o,air}$ (m^3/h)	1500
Indoor air volume flow $\dot{V}_{i,air}$ (m^3/h)	1000
Compressor electrical efficiency η_{el}	0.95 [14]
IHX efficiency η_{IHX}	0.3
Isentropic efficiency of each part of ejector	η_{mn}= 0.85, η_{sn}= 0.85, η_m= 0.9 and η_d= 0.85 [10]

Table 4. Performance comparison under rated cooling and heating conditions.

Mode	Parameters	CVCC	DEEC
Cooling	Compressor pressure ratio	2.14	1.8
	Evaporation temperature T_e	T_e=9.34 °C	$T_{e,MT}$=16.5 °C，$T_{e,LT}$=6.5 °C
	COP_c	2.77	3.57
	Exergy efficiency η_{ex}	27.2%	32.5%
Heating	Compressor pressure ratio	2.63	2.37
	COP_h	4.3	4.8
	Exergy efficiency η_{ex}	44.3%	49%

4.1. Energy performance analysis

4.1.1. Cooling mode

Fig. 4 illustrates the variation in cycle performance with compressor discharge pressure under cooling mode. As the discharge pressure increases, the COP_c of both cycles first rises and then declines, while the improvement ratio of COP_c for DEEC over CVCC gradually decreases. This diminishing improvement occurs because a lower discharge pressure results in greater throttling losses at a constant gas cooler outlet temperature. Under these conditions, the ejector in the DEEC effectively recovers expansion work, thereby significantly enhancing performance. At a discharge pressure of 9 MPa, the COP_c improvement ratio reaches 32.4%. Additionally, a higher discharge pressure increases the primary flow pressure, leading to higher fluid velocity at the nozzle outlet, which enhances the ejector's entrainment capability. Specifically, as the discharge pressure rises from 9 MPa to 11.4 MPa, the entrainment ratio increases from 0.25 to 0.4.

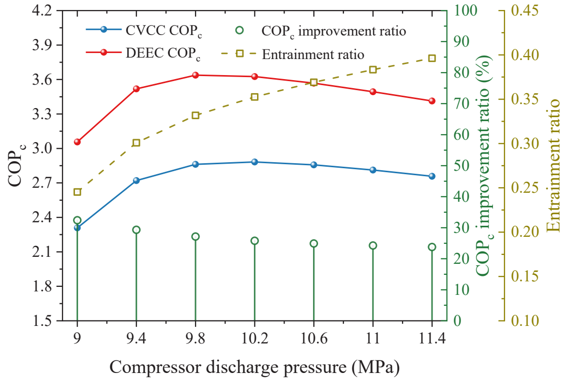

Figure 4. Variation of COP_c, COP_c improvement ratio and ejector 1 entrainment ratio with compressor discharge pressure.

The variations in cycle performance with IHX effectiveness and cooling load under cooling mode are presented in Fig. 5. As shown in Fig. 5(a), the COP_c increases with IHX effectiveness, which can be attributed to the corresponding rise in refrigerant subcooling. Furthermore, under a constant discharge pressure, greater subcooling reduces the irreversibility of the throttling process. Consequently, the relative advantage of the DEEC diminishes, leading to a decrease in the COP_c improvement ratio. Specifically, as the IHX effectiveness increases from 0.1 to 0.9, the COP_c improvement ratio declines from 30.6% to 22.9%, while the ejector entrainment ratio increases from 0.29 to 0.37.

As depicted in Fig. 5(b), under constant ambient temperature, an increase in the cooling load leads to a decrease in both the evaporation temperature and the COP_c. Under these conditions, the benefit provided by the ejector in the DEEC becomes more pronounced due to the increased irreversibility in the throttling process at higher loads, thereby enhancing its relative performance advantage. However, the reduction in evaporation temperature means a decrease in secondary flow pressure, which weakens the performance of the ejector. Specifically, as the cooling load increases from 3 kW to 6 kW, the COP_c improvement ratio rises from 24.3% to 30.2%, while the ejector entrainment ratio decreases from 0.37 to 0.29.

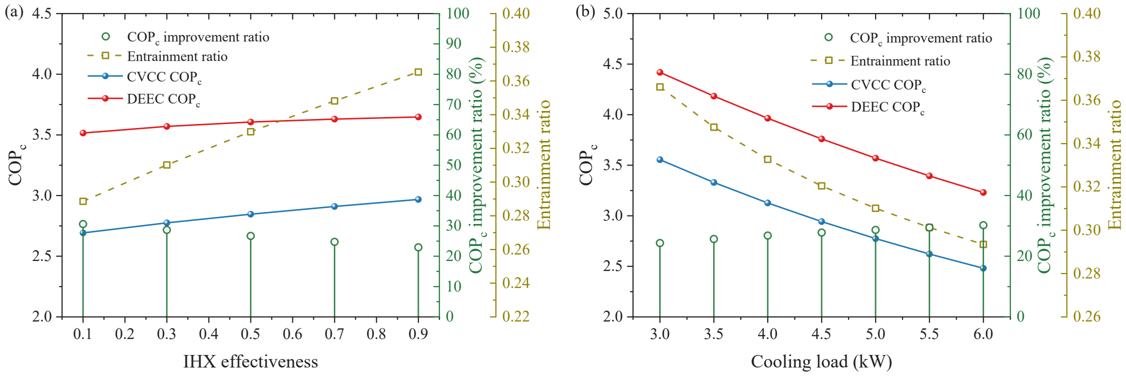

Figure 5. Variation of COP_c, COP_c improvement ratio and ejector 1 entrainment ratio with (a) IHX effectiveness and (b) cooling load under cooling mode.

4.1.2. Heating mode

Fig. 6 presents the variations in cycle performance with evaporation temperature and indoor ambient temperature under heating mode. As the evaporation temperature increases, the power consumption decreases, leading to an increase in the COP_h. However, the increase in evaporation temperature reduces throttling losses, which in turn diminishes the benefit of ejector. Consequently, the performance superiority of DEEC over CVCC diminishes at higher evaporation temperatures. Besides, a higher evaporation temperature means a higher secondary flow pressure, leading to a larger pressure difference across the suction chamber and thus improving the ejector performance.

As shown in Fig. 6(b), with the indoor ambient temperature increasing from 12 °C to 24 °C, the COP_h of both CVCC and DEEC decreases from 4.8 to 3.95 and from 5.23 to 4.50, respectively, while the COP_h improvement ratio increases from 8.8% to 13.9%. An increase in indoor temperature leads to a higher gas cooler outlet temperature, which results in greater irreversibility during the throttling process at a constant discharge pressure. This makes the effect of ejector on expanding work recovery more significant. Additionally, the entrainment ratio declines as the indoor temperature rises. Specifically, it drops from 0.83 to 0.67 as the indoor temperature increases from 12 °C to 24 °C.

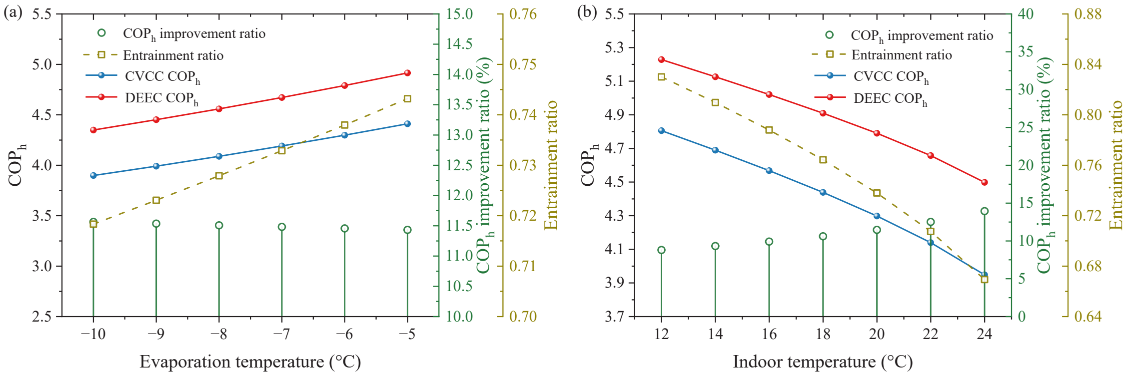

Figure 6. Variation of COP_h, COP_h improvement ratio and ejector 2 entrainment ratio with (a) evaporation temperature and (b) indoor temperature under heating mode.

4.2. Exergy performance analysis

4.2.1. Cooling mode

Fig. 7 illustrates the variations in the exergy destruction of various components in both the CVCC and DEEC with IHX effectiveness and cooling load under cooling mode. It can be observed that under all operating conditions, the exergy destruction in all components of the DEEC is consistently lower than that in the CVCC, corresponding to a significant reduction in the total cycle exergy destruction. This is primarily attributed to the introduction of the ejector, which substantially reduces the irreversibility of the throttling process, coupled with the optimized dual-temperature evaporation design that minimizes heat transfer irreversibility in the evaporator. Collectively, these improvements lead to a lower compressor pressure ratio and discharge temperature, thereby reducing exergy destruction in both the gas cooler and the compressor.

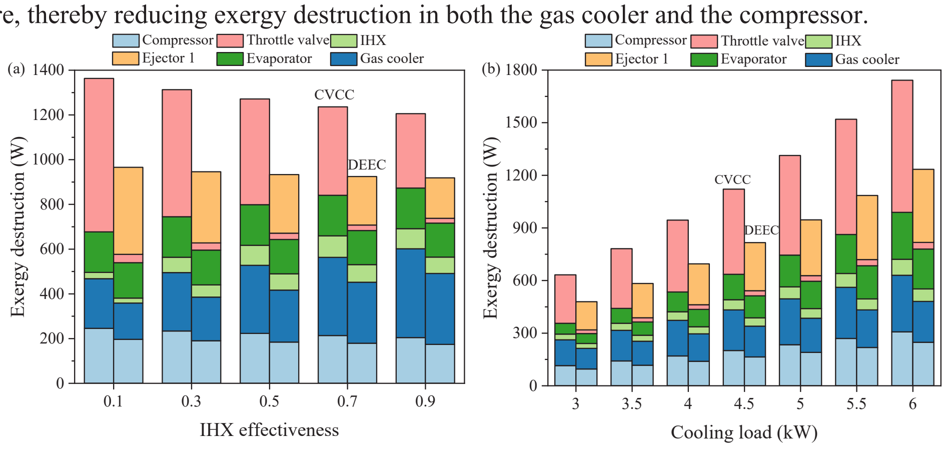

Figure 7. Variation of exergy destruction of the components with (a) IHX effectiveness and (b) cooling load under cooling mode.

As shown in Fig. 7(a), the exergy destruction of the expansion device decreases markedly with increasing IHX effectiveness, whereas the exergy destruction of the IHX and the gas cooler increases. Simulation results indicate that as the IHX effectiveness rises from 0.1 to 0.9, the exergy efficiency of the CVCC increases from 26.6% to 28.4%, while that of the DEEC increases from 32.1% to 33.0%, the improvement ratio of exergy efficiency for DEEC over CVCC reduced from 20.7% to 16.2%. Furthermore, as depicted in Fig. 7(b), an increase in cooling load leads to a decrease in evaporation temperature, resulting in increased exergy destruction across various components to different degrees. Despite this, the exergy efficiency of both cycles increases with the rising cooling load. Specifically, the exergy efficiency of the CVCC and DEEC increases from 25.1% to 28.0% and from 29.5% to 33.6%, respectively. Consequently, the improvement ratio of exergy efficiency rises from 17.5% to 20.0%.

4.2.2. Heating mode

Fig. 8 illustrates the variations in the exergy destruction of various components in both the CVCC and DEEC with evaporation temperature under cooling mode. Under identical operating conditions, the exergy destruction of the expansion device in DEEC is significantly lower than that in the CVCC, corresponding to a notably smaller total cycle exergy destruction, which aligns with the cooling mode. As the evaporation temperature increases, the exergy destruction in all cycle components decreases, and the exergy efficiency increases. Specifically, as the evaporation temperature rises from -10 °C to -5 °C, the exergy efficiency of the CVCC increases from 40.3% to 45.5%, with an exergy efficiency improvement ratio up to 11.2%.

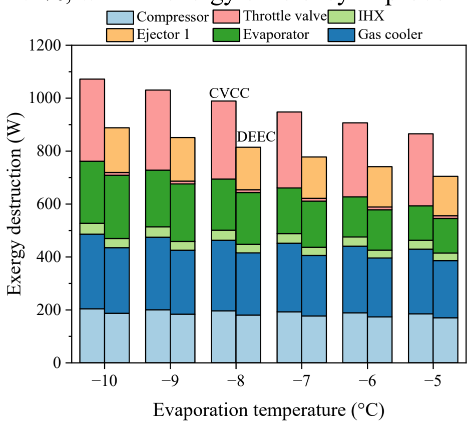

Figure 8. Variation of exergy destruction of the components with evaporation temperature under heating mode.

The exergy analysis confirms that the throttle valve is one of the primary sources of exergy destruction in the CVCC in both cooling and heating modes. In contrast, the DEEC effectively reduces irreversibility in this process through the incorporation of the ejectors in both modes, thereby achieving higher exergy efficiency. Within the parameter range studied in this paper, the DEEC demonstrates an exergy efficiency improvement of 10.6% to 20.7% compared to the CVCC.

5. Conclusions

This study presents a novel CO_2 dual-mode ejector-enhanced cycle (DEEC) designed to meet the demand for year-round efficient cooling and heating in applications such as building spaces and vehicles. A comparative analysis against the conventional vapor compression cycle (CVCC) was conducted based on energy and exergy analysis. The main conclusions are as follows:

(1) Under rated conditions, the coefficient of performance for cooling (COP_c) and heating (COP_h) of DEEC are increased by 28.9% and 11.6%, respectively, compared with CVCC. Meanwhile, the exergy efficiency is increased by 19.5% and 10.6% accordingly.

(2) Energy analysis reveals that in the cooling mode, the COP_c improvement ratio of the DEEC over the CVCC decreases with increasing compressor discharge pressure and IHX effectiveness, and increases with rising cooling load. Under the specified conditions, the improvement ratio reaches 22.9%–32.4%. In the heating mode, the COP_h improvement ratio decreases with increasing evaporation temperature and increases with rising indoor temperature, with an improvement range of 8.8%–13.9%.

(3) Exergy analysis demonstrates that the total exergy destruction of the DEEC is consistently and significantly lower than that of the CVCC under all operating conditions, with higher exergy efficiency. Within

the investigated parameter range, the improvement ratio of exergy efficiency for the DEEC over the CVCC reaches 10.6%–20.7%.

Nomenclature			
Symbols		B	back pressure
A	heat transfer area, m^2	c	cooling
c	velocity, m/s	cal	calculation
c_p	specific heat capacity, kJ/(kg·K)	com	compressor
h	specific enthalpy, kJ/kg	d	diffuser
$\dot{I}$	exergy destruction, W	e	evaporator
$\dot{m}$	mass flow rate, kg/s	el	electricity
P	pressure, MPa	ex	exergy analysis
$\dot{Q}$	heat transfer rate, kW	exp	experiment
s	specific entropy, kJ/(kg·K)	h	heating
T	temperature, °C	i	each component/indoor
U	heat transfer coefficient, kW/(m^2·K)	IE	indoor heat exchanger
$\dot{V}$	volumetric flow rate, m^3/h	IHX	internal heat exchanger
$\dot{W}$	work, kW	in	inlet
Abbreviation		is	isentropic process
COP	coefficient of performance	LT	low-temperature
CR	compression ratio	m	mixing chamber
CVCC	conventional vapor compression cycle	mn	motive nozzle
DEEC	dual-mode ejector-enhanced cycle	MT	medium-temperature
Greeks		o	outdoor
Δ	difference	out	outlet
μ	entrainment ratio	p	primary flow
η	efficiency	s	secondary flow
Subscripts		sn	suction nozzle
amb	ambient	tot	total

References

[1] Zhang X, Li Y. A review of recent research on hydrofluoroolefin (HFO) and hydrochlorofluoroolefin (HCFO) refrigerants. Energy. 2024;311. https://doi.org/10.1016/j.energy.2024.133423.
[2] Bani Issa AA, Liang C, Groll EA, Ziviani D. Residential heat pump and air conditioning systems with propane (R290) refrigerant: Technology review and future perspectives. Applied Thermal Engineering. 2025;266. https://doi.org/10.1016/j.applthermaleng.2025.125560.
[3] Boumaraf L, Haberschill P, Lallemand A. Investigation of a novel ejector expansion refrigeration system using the working fluid R134a and its potential substitute R1234yf. International Journal of Refrigeration. 2014;45:148-159. https://doi.org/10.1016/j.ijrefrig.2014.05.021.
[4] Eskandari Manjili F, Cheraghi M. Performance of a new two-stage transcritical CO2 refrigeration cycle with two ejectors. Applied Thermal Engineering. 2019;156:402-409. https://doi.org/10.1016/j.applthermaleng.2019.03.083.
[5] Wen Z, Bai T, Wan J. Thermodynamic analysis of a modified transcritical CO2 two-stage compression dual-temperature refrigeration cycle with an ejector. Applied Thermal Engineering. 2024;257. https://doi.org/10.1016/j.applthermaleng.2024.124383.
[6] Cen J, Liu P, Jiang F. A novel transcritical CO2 refrigeration cycle with two ejectors. International Journal of Refrigeration. 2012;35(8):2233-2239. https://doi.org/10.1016/j.ijrefrig.2012.07.001.
[7] Wang Y, Yin Y, Cao F. Comprehensive evaluation of the transcritical CO2 ejector-expansion heat pump water heater. International Journal of Refrigeration. 2023;145:276-289. https://doi.org/10.1016/j.ijrefrig.2022.09.008.
[8] Xing M, Yu J, Liu X. Thermodynamic analysis on a two-stage transcritical CO 2 heat pump cycle with double ejectors. Energy Conversion and Management. 2014;88:677-683. https://doi.org/10.1016/j.enconman.2014.09.025.
[9] Zou Y, Liu F, He J, Mao S, Jiao Q, Zhao X, et al. Comprehensive evaluation and optimization of IHX in a modified double-evaporator transcritical CO2 heat pump with ejector. Energy. 2025;335. https://doi.org/10.1016/j.energy.2025.137815.
[10] Wang Z, Fan M, He G, Song H, Yang W. Performance analysis of a double-efficient CO2 cooling and heating system using an ejector. Applied Thermal Engineering. 2023;227. https://doi.org/10.1016/j.applthermaleng.2023.120434.
[11] Dai B, Yang P, Liu S, Zhao R, Li X, Wang X. Annual space heating and cooling carbon dioxide system based on hybrid techniques of ejector and integrated mechanical subcooling: Optimization and energy, exergy, environment and economic evaluation throughout the world. Energy Conversion and Management. 2025;332. https://doi.org/10.1016/j.enconman.2025.119749.
[12] Cao X, Liang X, Shao L, Zhang C. Performance analysis of an ejector-assisted two-stage evaporation single-stage vapor-compression cycle. Applied Thermal Engineering. 2022;205. https://doi.org/10.1016/j.applthermaleng.2021.118005.

[13] Zhu Y, Li C, Zhang F, Jiang P-X. Comprehensive experimental study on a transcritical CO 2 ejector-expansion refrigeration system. Energy Conversion and Management. 2017;151:98-106. https://doi.org/10.1016/j.enconman.2017.08.061.
[14] Zarei A, Zaboli S, Babaie Rabiee M. Energy and exergy analysis of a high-efficiency multi-evaporator absorption refrigeration system with integrated ejectors and compression cooling system. Applied Thermal Engineering. 2025;267. https://doi.org/10.1016/j.applthermaleng.2025.125753.